ELSEVIER

Polymer 42 (2001) 3751–3759

polymer

www.elsevier.nl/locate/polymer

Reactive compatibilization of nylon 6/styrene–acrylonitrile copolymer blends
Part 3. Tensile stress–strain behavior

N. Kitayama[1], H. Keskkula, D.R. Paul*

Department of Chemical Engineering and Center for Polymer Research, The University of Texas at Austin, Austin, TX 78712, USA

Received 23 May 2000; received in revised form 5 September 2000; accepted 27 September 2000

Abstract

The stress–strain behavior of blends of nylon 6 (PA) and a styrene–acrylonitrile copolymer (SAN) compatibilized by an imidized acrylic polymer (IA) was evaluated in terms of the IA content and the dispersed SAN25 particle size. PA/SAN blends can be considered as a simpler version of industrially important PA/ABS blends; therefore, this study provides better understanding of the stress–strain behavior of compatibilized PA/ABS blends. The IA content was varied from 0 to 5 wt%; whereas the ratio of PA to SAN25 was held at 7/3; and in all cases the polyamide formed the continuous phase. From experiments using a Brabender batch mixer or an extruder as the mixing device, a reduction of dispersed particle size was observed with the addition of as little as 0.1 wt% IA. It was revealed from the experiments using a Brabender batch mixer that more than 0.5 wt% IA was necessary to prevent domain coalescence. The blends containing 1 wt% or more IA show necking and considerable plastic deformation. Transmission electron microscopy revealed that the normally brittle SAN25 particles were transformed into elongated shapes and undergo shear yielding under certain circumstances as the specimens experienced plastic deformation during stress–strain testing. Although the macroscopic elongation at break and the particle distortion ratio, which is defined as the ratio of the major axis to the minor axis of the elongated particles, are somewhat correlated, the local deformation in the neck region is much larger than the elongation at break. Thus, the ultimate capability for plastic deformation of the IA compatibilized blends is much larger than the overall elongation at break. The distortion ratio of the particles was observed to be as high as 6–7. There seems to be a relationship between the SAN25 particle size and the extent of plastic deformation realized. These experiments, however, do not differentiate the effect of diminishing particle size from increasing adhesion between the phases. Thus, it is not possible to assign unambiguously the dominant factor that permits the plastic deformation of the brittle SAN phase.

Keywords: Nylon 6; Styrene–acrylonitrile copolymer; Imidized acrylic polymer

1. Introduction

Parts 1 and 2 [1,2] of this series explored the effect of reactive compatibilization on the phase inversion behavior and the relationship between the dispersed phase particle size and composition for nylon 6 blends with a styrene–acrylonitrile copolymer (SAN). Studies on this simple blend system provide a basis for a better understanding of morphology development in the commercially important [3–9] but more complex blends of polyamides with ABS materials. The range of compositions where each component forms dispersed particles and the intermediate region of co-continuous morphologies were established in different mixing devices, with and without an imidized acrylic polymer (IA) or a styrene/acrylonitrile/maleic anhydride terpolymer (SANMA) compatibilizer. For blends without a compatibilizer, the domain size of the dispersed phase increases as the minor phase concentration increases, and the relation between domain size and composition shows a symmetric trend about the phase inversion composition. For a batch mixer, the reactive compatibilizers significantly decrease the size of the SAN dispersed particles in the nylon 6 matrix especially near the point of phase inversion; whereas, beyond the point of phase inversion, the domains of nylon 6 exist as relatively large particles in the SAN matrix. It seems that the compatibilizer is not so effective in reducing domain size on this side of the phase inversion composition. That is, the relation between domain size and the composition for the compatibilized blends shows an asymmetric relationship about the region of phase inversion.

* Corresponding author. Tel.: + 1-512-471-5392; fax: +1-512-471-0542.

E-mail address: drp@che.utexas.edu (D.R. Paul).

[1] Permanent address: Mitsubishi Gas Chemical Co. Inc. Mitsubishi Building, 5-2, Marunouchi 2-chome, Chiyoda-ku, Tokyo 100-005, Japan.

0032-3861/01/$ - see front matter
PII: S0032-3861(00)00695-9

The purpose of this paper is to explore the effect of reactive compatibilization via the imidized acrylic polymer on the tensile stress–strain behavior of nylon 6 blends with SAN25. Previous studies [10–34] suggest that under certain conditions polymers which usually show brittle fracture may exhibit ductile behavior in blends or multi-layer structures. The blends of interest here have a matrix (nylon 6) that is generally ductile with a dispersed phase (SAN copolymer) that is usually brittle. The adhesion between nylon 6 and the SAN copolymer is relatively poor; however, the addition of imidized acrylic as a compatibilizer improves the adhesion between a nylon 6 phase and SAN phase. It is shown that these blends exhibit a high level of macroscopic plastic deformation during measurement of stress–strain diagrams when the blend contains more than a certain IA content. It seems that there is a relationship between the dispersed SAN particle size and the extent of elongation exhibited by the blend; however, these experiments do not differentiate the effect of diminishing particle size from increasing adhesion between the phases. Thus, it is not possible to assign unambiguously the dominant factor that permits the plastic deformation of the brittle SAN phase.

2. Experimental

All materials and experimental procedures were identical to those used in the previous papers in this series [1,2]. Three nylon 6 materials with low (L-PA, $\bar{M}_n = 16,700$), medium (M-PA, $\bar{M}_n = 22,000$), and high (H-PA, $\bar{M}_n = 29,300$) molecular weight were used as the matrix. The SAN contained 25 wt% AN by weight and is designated as SAN25 ($\bar{M}_w = 152,000$).

Blends were prepared by simultaneous extrusion of all components in a Killion single-screw extruder ($L/D = 30$, $D = 25.4$ mm), outfitted with an intensive mixing head, at 240°C using a screw speed of 40 rev/min. The extrudate was immediately drawn through a water bath and pelletized. All materials were dried in a vacuum oven at 80°C for at least one day prior to all melt mixing. The extrudate was injection molded into standard tensile bars of 3.18 mm thickness (ASTM D638 type I) using an Arburg Allrounder injection molding machine at the temperature of 240°C. The molding parameters were kept identical for all samples. For comparison, some blends were prepared in a Brabender as described previously [1,2].

Stress–strain diagrams at ambient temperature were obtained using an Instron 1137 with a crosshead speed of 5.08 cm/min to establish the elongation at break, and 0.508 cm/min to determine the modulus and yield or fracture stress. All specimens were inspected prior to the test and any with obvious imperfections were discarded. A series of five specimens were tested for each blend, and the average value is reported here. However, the elongation at break is generally more variable for highly ductile blends; therefore, apparent premature failures were omitted from the calculation of the average value. The unusually lower elongation value at break might be attributed to imperfections not visible to the naked eye.

The conditions for cryogenically microtomy and transmission electron microscopy (TEM) are provided elsewhere [1]. Sections for particle size analysis were taken from various positions across the thickness of tensile bars in directions perpendicular and parallel to the flow direction of injection molding. More than 200 particles were measured to determine the average domain size.

3. Results

3.1. Effect of IA polymer content on SAN25 particle size

Fig. 1 shows the relationship between the weight average SAN25 particle diameter, $\bar{d}_w$, and the content of IA in 70/30 M-PA/SAN25 blends prepared in a Brabender batch mixer (filled circles) and in a single screw extruder followed by injection molding to form tensile test specimens (open circles). The size of the dispersed phase particles were calculated from TEM photomicrographs of sections cut from a plane parallel to the flow direction of the injection molding. The ratio of M-PA to SAN25 was kept at 7/3 in all cases, e.g. the composition of the blend compatibilized with 5 wt% IA compatibilized blend is M-PA/SAN25/IA = 66.5/28.5/5 on a weight basis. It is seen that the dispersed SAN25 particle size decreases, but in somewhat different ways depending on the method of mixing, as the IA content increases. A significant reduction in particle size is noted at compatibilizer content as low as 0.1 wt%. This indicates that only a small amount of graft copolymer is needed to have a measurable effect on the interfacial characteristics of the blend. The use of a single screw extruder can be more effective for attaining a fine dispersion of the SAN25 phase, especially at the higher IA content. The extruder provides more intensive mixing

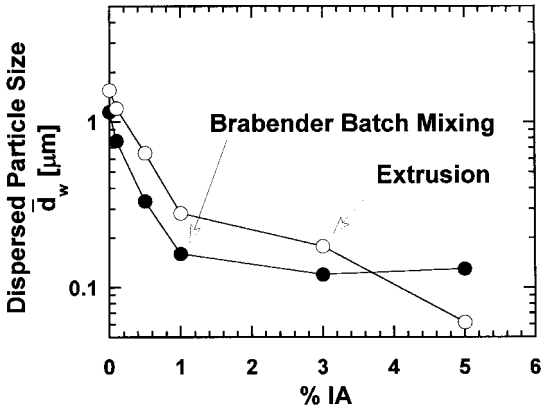

Fig. 1. Reduction of dispersed SAN25 particle size due to the addition of IA: comparison between Brabender batch mixing and extrusion for 70/30 M-PA/SAN25 blends.

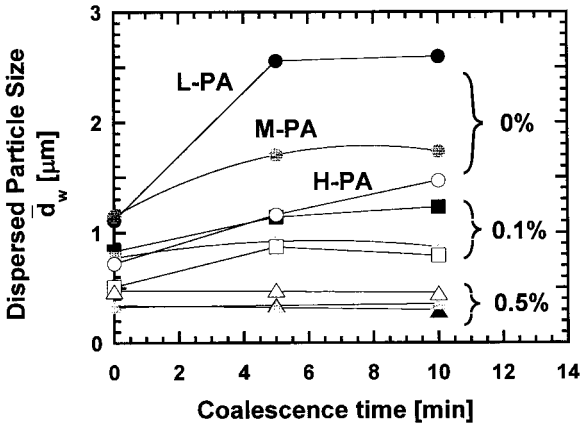

Fig. 2. Growth of the dispersed SAN25 particle size due to coalescence as a function of IA content for blends based on three different molecular weight nylon 6 using Brabender batch mixer protocol described in text.

than the Brabender batch mixer does; however, the residence time in the extruder is much shorter (~3 min) than in the batch mixer (~10 min) for this series of experiments. The longer residence time may explain why the batch mixer gives a finer dispersion than the extruder at low IA contents.

3.2. Effect of compatibilizer content for stabilization of blend morphology

The minimum quantity of IA for stabilizing blend morphology has been estimated for blends of SAN with three different molecular weights of nylon 6. The blend composition was fixed at PA/SAN25 = 70/30 in all cases. Fig. 2 shows that the dispersed SAN25 particle size for the three blends (with and without IA) grows with time due to domain coalescence. The protocol for this experiment is described below.

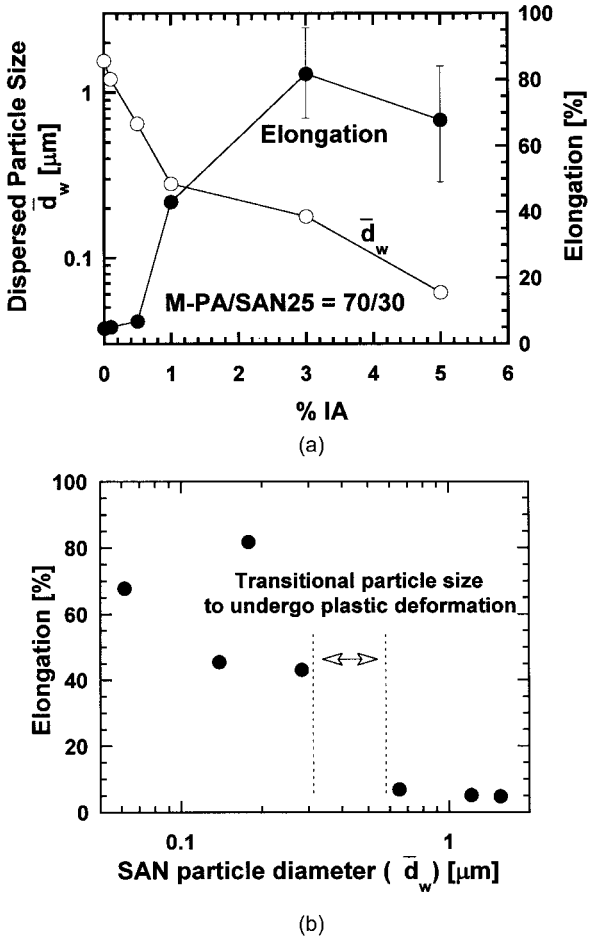

Fig. 4. (a) Effect of IA content on elongation at break and the inverse correlation between elongation at break and weight average SAN25 particle size for 70/30 M-PA/SAN25 blends. (b) Relation between dispersed SAN25 particle size and elongation at break for 70/30 M-PA/SAN25 blends compatibilized with IA.

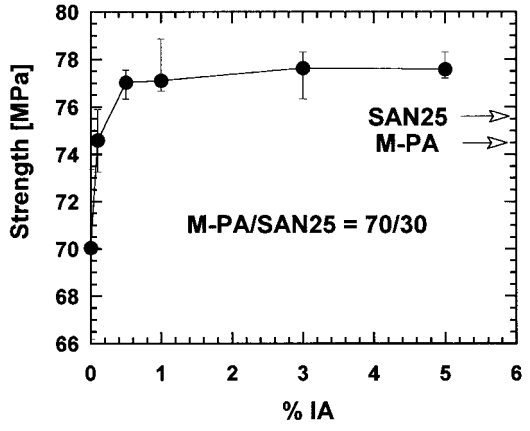

Fig. 3. Effect of the IA content on the yield (≥1% IA) or fracture strength (<1% IA) for 70/30 M-PA/SAN25 blends. Arrows show tensile strength of pure SAN25 and pure M-PA (at yield) for reference.

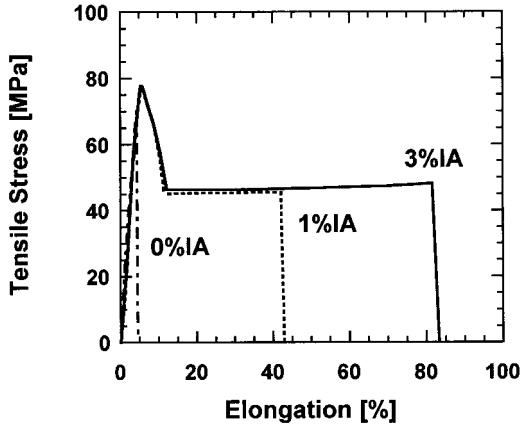

Fig. 5. Effect of the IA content on the stress–strain diagrams of 70/30 M-PA/SAN25 blends.

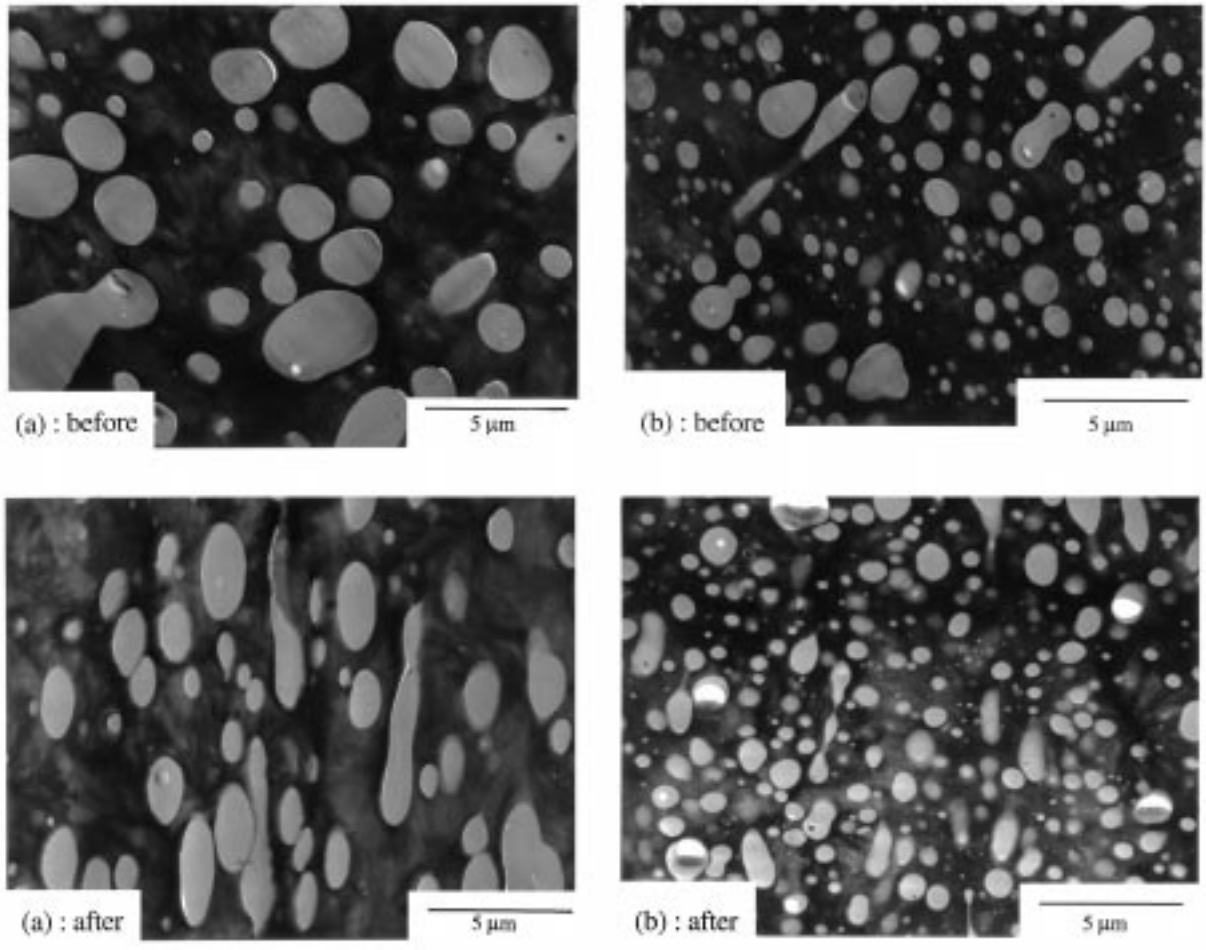

Fig. 6. (a) TEM photomicrographs showing the morphology of 70/30 M-PA/SAN25 blends compatibilized with 0 wt% , (b) 0.5 wt%, (c) 1 wt%, (d) 3 wt%, and (e) 5 wt% IA, from molded specimens (before tensile testing) and from the necked region (after tensile testing).

Sixty grams of mechanically pre-mixed pellets of this composition were introduced into the Brabender (preheated to 240°C) and mixed at 60 rev/min for 10 min; the particle size attained is indicated at zero coalescence time in Fig. 2. Note that previous work showed that the average particle size becomes constant in less than 10 min of mixing [35]. At this point, the Brabender rotor speed was reduced to 5 rpm and samples were collected after 5 and 10 min for TEM analysis. The reduction in rotor speed alters the balance of drop break-up versus domain coalescence, i.e. the extent of drop break-up is reduced by lowering the shear rate while the rate of domain coalescence is less affected. The validity of this experiment for establishing the stabilization of morphology by reactive compatibilizers has been verified in the previous reports from our laboratory [35,36]. Growth of the domain size during the period of mixing at low shear rate indicates the extent of instability of the blend morphology.

The data in Fig. 2 show that the addition of 0.5 wt% or more of IA stabilizes the blend morphology for 70/30 PA/SAN25 blends regardless of the nylon 6 molecular weight. The addition of 0.1 wt% IA shows a little improvement of morphology stability. For uncompatibilized blends, domain coalescence is more rapid the lower the nylon 6 molecular weight; this may be attributed to the resulting lower melt viscosity.

3.3. Tensile stress–strain behavior

Since both nylon 6 and SAN materials break in a brittle manner during high speed mechanical tests, e.g. Izod impact test, the blends of a nylon 6 with SAN also show brittle behavior regardless of the addition of a compatibilizer (see Table 1). Thus, slow speed tensile tests are more appropriate for determining the effects of compatibilization on

Table 1

Composition	Izod [J/m]a[a]
Nylon 6, M-PA	56
SAN25	22
M-PA/SAN25 = 70/30	32
M-PA/SAN25/IA = 66.5/28.5/5	31

[a] At ambient temperature.

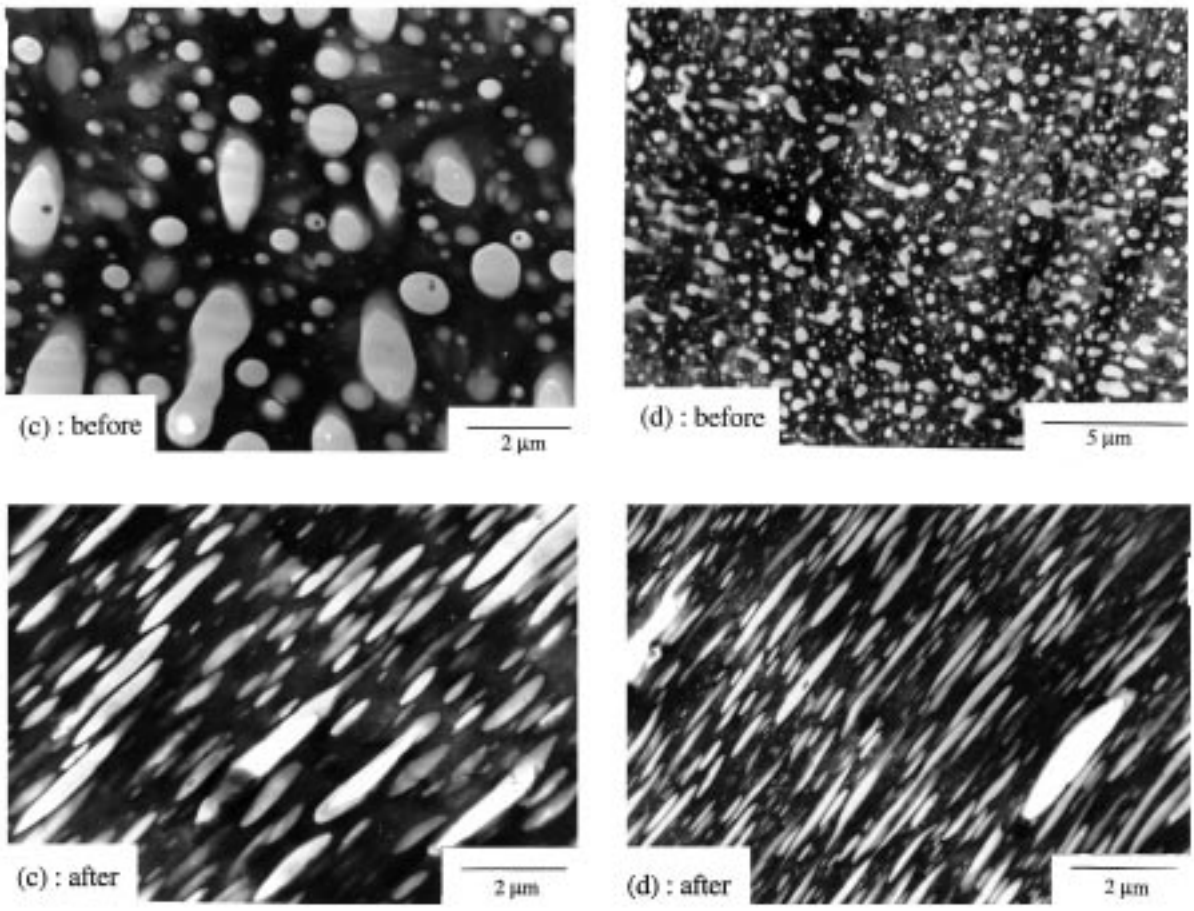

Fig. 6. (*continued*)

macroscopic ductility of these blends. Nylon 6 shows ductile behavior during slow speed deformation, i.e. high elongation prior to breaking, while SAN materials break before yielding, i.e. a low elongation at break. This contrast of elongation characteristics of the two materials is a key factor in the following.

The blend modulus for these blends is essentially independent of IA content within the limits used here, i.e. the average modulus for these blends shows a constant value of 2.94 MPa ($\sigma = 0.08$) as the IA content was varied from 0 to 5 wt%. Addition of significantly larger amounts of IA would be expected to raise the blend modulus [10–14,32].

Fig. 3 shows the effect of IA content on the stress at break for 70/30 M-PA/SAN25 blends. The arrows on the right show the yield strength of pure M-PA and the fracture stress of pure SAN25. Without any IA, the strength of the blend is much lower than that of either pure M-PA or SAN25. This may reflect poor adhesion between the phases. The addition of more than 0.5 wt% IA leads to ductile materials whose yield strength reaches a plateau value that exceeds the fracture strength of pure SAN25 and the yield strength of M-PA. Fig. 4a shows the effect of IA content on the elongation at break of these blends. There seems to be an inverse correlation between the elongation at break and the SAN25 particle size. When the IA content is below 1 wt%, the blends break before yielding. Above 1 wt% IA, the dispersed SAN25 particles become smaller, and the blends begin to elongate beyond the yield point. Although the values of elongation at break for nylon 6/SAN25 blends compatibilized with more than 1 wt% IA are smaller than those of pure nylon 6 (>200%), the tensile behavior exhibited by these blends is typical of nylon 6 materials in terms of sample necking in spite of the substantial content of the normally brittle SAN25. Fig. 4b suggests there is a relationship between the elongation at break for the blends studied here and the dispersed SAN25 particle size regardless of the blend composition or the IA content of the blend. It appears that the particle size must be below a critical value for the blend to exhibit plastic deformation. When the particle size exceeds this critical size range of 0.3–0.6 μm, the blends break in a brittle manner without yielding. Fig. 5 illustrates the effect of IA content on the deformation mode of nylon 6/SAN25 blends. Without IA compatibilization, the blends break before yielding; whereas, for blends containing more than 1 wt% IA, stable plastic deformation beyond neck formation occurs. As seen here, the elongation at break is even larger at 3 wt% IA.

The TEM photomicrographs in Fig. 6 show the morphology of 70/30 M-PA/SAN25 blends compatibilized with

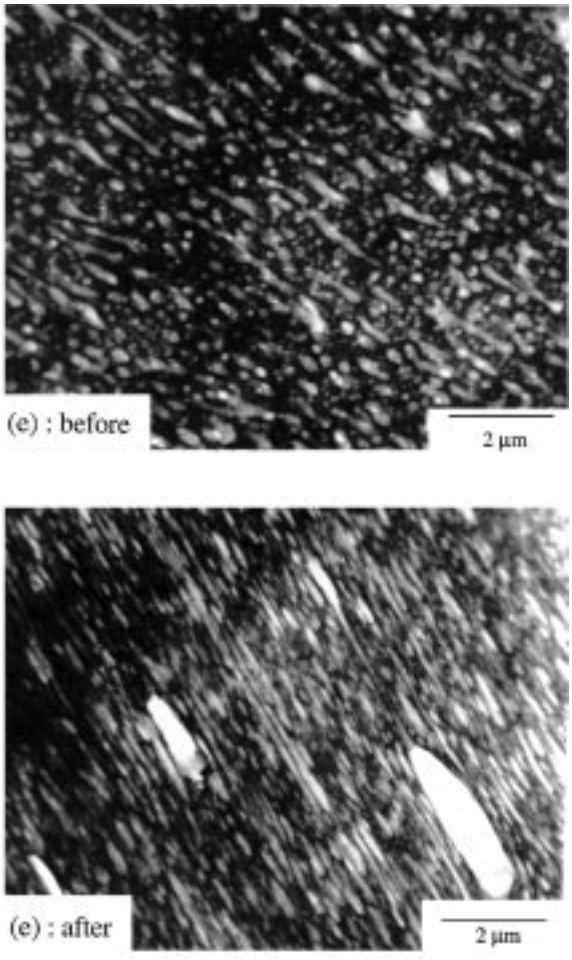

Fig. 6. (*continued*)

progressively larger amounts of IA before and after the tensile test. The pictures shown were taken from the center of the ASTM D638 type I specimens (dog bone specimen) parallel to the flow direction during injection molding. The well compatibilized, ductile blends showed a nearly uniform morphology across the sample thickness.

For blends containing less than 0.5 wt% IA that break before yielding, the SAN particle shape is essentially the same before and after the tensile test. However, for the blends compatibilized with 1 wt% or more IA that are ductile, considerable plastic deformation of the dispersed SAN25 particles occurs during the tensile test, i.e. the essentially circular particles in the as-molded blend deform into an elliptic shape during the tensile test. The extent of particle distortion is even greater than might be expected from the observed macroscopic deformation as shown later. Note that some of the relatively large particles in these blends are not transformed into an elongated shape. As a result, some voids emerge behind the elongated particles, e.g. the white areas in Fig. 6c (after).

A particle distortion ratio, (DR), can be defined as

$$\mathrm{DR} = (a_1/b_1)/(a_0/b_0), \tag{1}$$

where a and b are the major and minor axes of the dispersed particle, and the subscripts 0 and 1 indicate values prior to and after the tensile test, respectively, see Fig. 7.

Fig. 8 shows that the elongation at break and this particle DR, follow a similar trend as the IA content of the blend is varied. The distortion ratio was calculated by averaging many values (more than 100) from TEM photomicrographs.

The particle DR is replotted in Fig. 9 versus the overall draw ratio at break for the macroscopic test bar, i.e. draw ratio = 1 + %Elongation at break/100. Ideally, the particle distortion ratio should be equal to the macroscopic draw ratio of the specimen, i.e. the dotted line. However, the extent of particle distortion is significantly greater than the maximum macroscopic draw ratio since the data lie significantly above the dotted line in Fig. 9. This, of course, is due to the fact that the sample breaks prior to the neck propagating throughout the entire gauge section of the specimen. That is, the local deformation in the necked region is much larger than indicated by the observed elongation at break, see Fig. 10. This means that the ultimate capability of blends compatibilized with more than 1 wt% IA to undergo plastic deformation is much greater than the measured elongation at break.

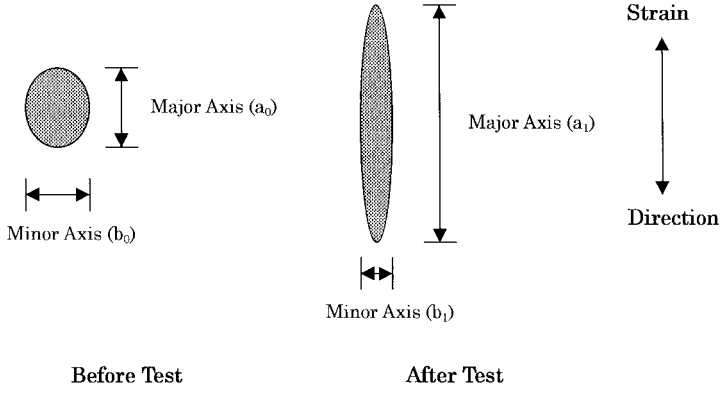

Fig. 7. Illustrative comparison of the dispersed SAN25 particles before and after tensile testing.

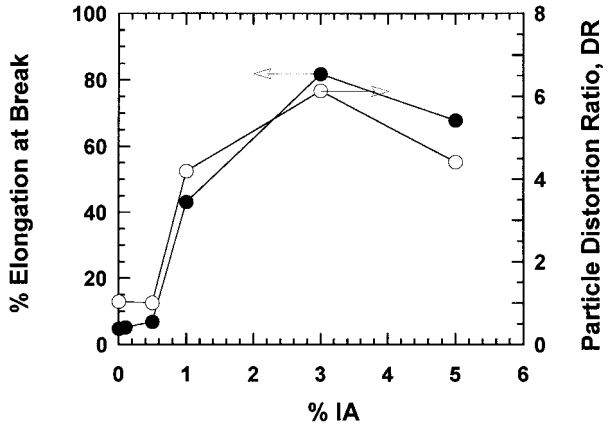

Fig. 8. Correlation between the tensile elongation at break and the particle DR, calculated from TEM photomicrographs.

The shear yielding which evidently occurs in well-dispersed SAN particles that are bonded to the nylon 6 matrix has significant ramifications. Such behavior has been noted previously and various mechanisms for this behavior have been discussed.

Fujita et al. [11], Kurauchi et al. [14], Keitz et al. [32], Wildes et al. [35], and Koo et al. [12], have shown that polycarbonate blends with ABS and/or SAN copolymers can exhibit ductile fracture and achieve elongation in tensile tests even though SAN is typically a brittle material. Koo et al. [12] proposed that the normally brittle SAN undergoes cold drawing in such bends owing to a compressive stress on the equatorial plane of the particles which transforms the deformation mode from crazing to shear yielding. It is known that brittle materials may show ductile behavior under high enough hydraulic pressures. In studies of polystyrene (PS) multilayer films with polyethylene or poly(phenylene ether), Sanden et al. [29–31] showed that normally brittle PS shows ductile behavior when this layer is thinner below a critical thickness. Baer and co-workers

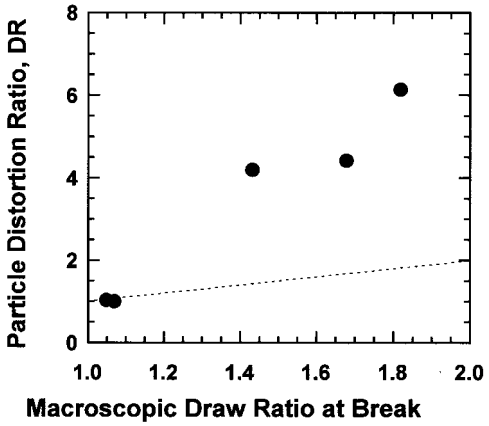

Fig. 9. Particle DR, versus the overall draw ratio at break for the macroscopic test bar, i.e. draw ratio = 1 + %Elongation at break/100.

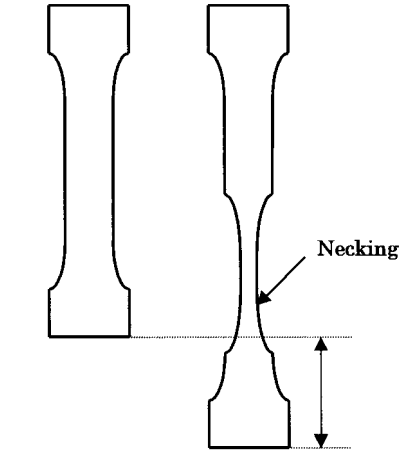

Fig. 10. Illustrative comparison of the tensile test specimens before and after the test. Note that the strain in the necked region is much larger than the measured macroscopic elongation at break.

[15–21] showed that the multilayers of PC/SAN become ductile when the thickness of each layer was decreased below a critical level. Although the generation of many crazes in SAN layers was seen, the extension of crazes was halted when the crazes met shear bands in the PC layers. This is due to the affinity between PC and SAN that leads to good adhesion between the layers. Baer and co-workers also studied the effect of compatibilizing agents on the cold drawing of incompatible blends, then showed the effect of the functionality, the amount, the molecular weight, and crystallinity of the compatibilizing agents [22–24]. Inoue and co-workers [10] compared the tensile behavior for

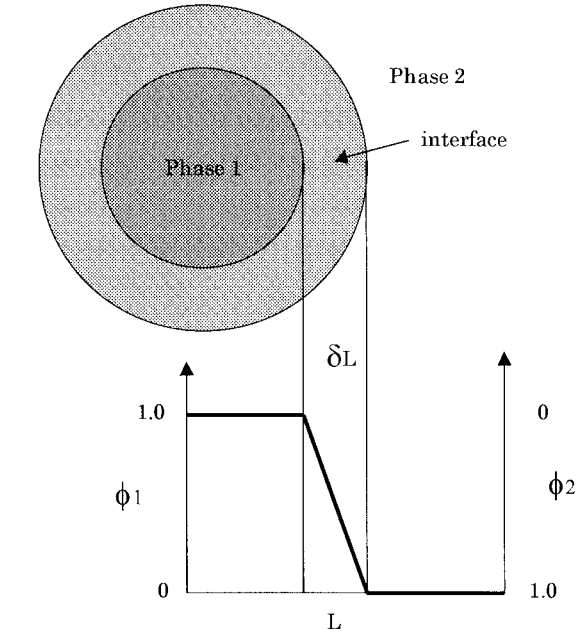

Fig. 11. Schematic representation of the interfacial region for a compatibilized blend [41].

nylon 6 blends with PS and/or styrene/maleic anhydride copolymer (SMA). It was shown that an increase in interfacial adhesion between a ductile nylon 6 matrix and a brittle dispersed component allowed plastic deformation of the brittle dispersed component, PS. Creton et al. [26], Armat et al. [27], and Adedeji et al. [28] also individually suggested that improving the interfacial adhesion between immiscible polymers by addition of compatibilizing agents leads to effective stress transfer between the incompatible phases. Harada et al. [13] studied ternary blends of nylon 6 toughened by particles of styrene/ethylene/butadiene/styrene rubber (SEBS-*g*-MA), or a maleated ethylene/propylene rubber (EPR-*g*-MA), and reinforced by rigid IA particles. In spite of the addition of the brittle IA material, the blends show ductile properties with the improved stiffness. This work points to some very significant benefits that result from the transition from brittle ductile deformation of rigid polymer phases as their phase size becomes small.

Another mechanistic possibility arises from the reactive nature of the IA particles. Inoue and co-workers [37–41] showed that reactively compatibilized blends can form a very thick interface (more than a few ten nm) between the phases. They propose that the in situ formed graft polymers reside in the interfacial region in the form of a smooth concentration gradient between phases. Fig. 11 shows a schematic representation of this interfacial region as visualized by Utracki [42], i.e. the structure of the dispersed particle is somewhat like a core/shell type material. For large particles, the interfacial layer is a negligible fraction of the material; however, as the particles become very small the interfacial region can become relatively more important. That is, the ratio of δL to the particle diameter may become significant and in the limit the particle becomes dominated by the interfacial region. In this case, the particle is really a mixture of materials and no longer has the properties of the original brittle material.

4. Conclusions

The stress–strain behavior of nylon 6 blends with SAN25 reactively compatibilized by an IA polymer was evaluated in terms of the IA content and the dispersed SAN25 particle size. The IA content was varied from 0 to 5 wt%; the ratio of M-PA to SAN25 was held at 7/3; and in all cases the polyamide formed the continuous phase.

A reduction of dispersed particle size was observed with the addition of as little as 0.1 wt% IA, while more than 0.5 wt% IA was necessary to prevent domain coalescence. The blends containing 1 wt% or more IA show necking and considerable plastic deformation. TEM revealed that the rigid SAN25 particles were transformed into elongated shapes as the specimens experienced plastic deformation during stress–strain testing. In other words, the normally brittle SAN25 particle undergoes shear yielding under proper circumstances. The macroscopic elongation at break and the particle distortion ratio are somewhat correlated. Actually the local deformation in the neck region is much larger than the elongation at break indicates, so the ultimate capability for plastic deformation of the IA compatibilized blends is much larger than the overall elongation at break. The distortion ratio of the particles was observed to be as high as 6–7. There seems to be a relationship between the SAN25 particle size and the extent of plastic deformation realized.

Acknowledgements

The authors express their appreciation to Mitsubishi Gas Chemical Co. Inc., and Mitsubishi Engineering-Plastics Corp. for their support of various aspects of this research.

References

[1] Kitayama N, Keskkula H, Paul DR. Polymer 2000;41:8041.
[2] Kitayama N, Keskkula H, Paul DR. Polymer 2000;41:8053.
[3] Lavengood RE, Padwa AR, Harris AF. U.S. Patent, 4 713 415, December 15 1987, (Monsanto).
[4] Lavengood RE, Patel R, Padwa AR. U.S. Patent 4 777 211, October 11 1988, (Monsanto).
[5] Lavengood RE, Patel R, Padwa AR. European Patent Application, 0220155, April 29 1987, (Monsanto).
[6] Baer M. U.S. Patent, 4 584 344, April 22 1986, (Monsanto).
[7] Miyake Y. Japanese Patent, 02240158-A, September 25 1990, (Daicel Chem. Ind. KK).
[8] Aoki Y, Watanabe M. U.S. Patent, 4 987 185, January 22 1991, (Monsanto Kasei Co.).
[9] Tomono H, Yamamoto I, Aoki Y. U.S. Patent, 4 981 906, January 1 1991, (Monsanto Kasei Co.).
[10] Angola JC, Fujita Y, Sakai T, Inoue T. J Polym Sci: Part B: Polym Phys 1988;26:807.
[11] Fujita Y, Koo KK, Angola JC, Inoue T, Sakai T. Kobunshi Ronbunshu 1986;43(3):119.
[12] Koo KK, Inoue T, Miyasaka K. Polym Engng Sci 1985;25:741.
[13] Harada T, Carone Jr E, Kudva RA, Keskkula H, Paul DR. Polymer 1999;40:3957.
[14] Kurauchi T, Ohta T. J Mater Sci 1984;19:1699.
[15] Gregory BL, Siegmann A, Im J, Hiltner A, Baer E. J Mater Sci 1987;22:532.
[16] Ma M, Vijayan K, Hiltner A, Baer E. J Mater Sci 1990;25:2039.
[17] Shin E, Hiltner A, Baer E. J Appl Polym Sci 1993;47:245.
[18] Shin E, Hiltner A, Baer E. J Appl Polym Sci 1993;47:269.
[19] Haderski D, Sung K, Im J, Hiltner A, Baer E. J Appl Polym Sci 1993;52:121.
[20] Ebeling T, Hiltner A, Baer E. J Appl Polym Sci 1998;68:793.
[21] Sung K, Haderski A, Hiltner A, Baer E. J Appl Polym Sci 1994;52:135.
[22] Sung K, Haerski D, Hiltner A, Baer E. J Appl Polym Sci 1994;52:147.
[23] Duvall J, Sellitti C, Myers C, Hiltner A, Baer E. J Appl Polym Sci 1994;52:195.
[24] Duvall J, Sellitti C, Myers C, Hiltner A, Baer E. J Appl Polym Sci 1994;52:207.
[25] Duvall J, Sellitti C, Topolkaraev V, Hiltner A, Baer E, Myer C. Polymer 1994;35:3948.
[26] Creton C, Kramer EJ, Hadziioannou G. Macromolecules 1991;24:1846.
[27] Armat R, Moet A. Polymer 1993;34:977.

[28] Adedeji A, Jamieson AM. Polymer 1993;34:5038.
[29] Sanden MCM van der, Meijer HEH, Lemstra PJ. Polymer 1993;34:2148.
[30] Sanden MCM van der, Buijs LGC, Bie FO de, Meijer HEH. Polymer 1994;35:2783.
[31] Sanden MCM, Meijer HEH. Polymer 1994;35:2991.
[32] Keitz JD, Barlow JW, Paul DR. J Appl Polym Sci 1984;29:3131.
[33] Lombardo BS, Keskkula H, Paul DR. J Appl Polym Sci 1994;54:1697.
[34] Stretz HA, Cassidy PE, Paul DR. J Appl Polym Sci 1999;74:1508.
[35] Wildes G, Keskkula H, Paul DR. J Polym Sci: Part B: Polym Phys 1999;37:71.
[36] Hale W, Keskkula H, Paul DR. Polymer 1999;40:365.
[37] Bhowmick AK, Chiba T, Inoue T. Polymer 1993;50:2055.
[38] Yukioka S, Inoue T. Polymer 1994;35:1182.
[39] Kressler J, Higashida N, Inoue T, Heckmann W, Seitz F. Macromolecules 1993;26:2090.
[40] Li H, Chiba T, Higashida N, Yang Y, Inoue T. Polymer 1997;38:3921.
[41] Dedecker K, Groeninckx G, Inoue T. Polymer 1998;39:5001.
[42] Utracki LA. Polymer alloys and blends: thermodynamics and rheology. Munich: Carl Hanser, 1990, 119 p.